



ISSN 1110-0451

# Arab Journal of Nuclear Sciences and Applications

Web site: [ajnsa.journals.ekb.eg](http://ajnsa.journals.ekb.eg)



(E S N S A)

## Neutronics Design Study of Nuclear Thermal Rocket using Low Enriched Uranium Fuel

Asma Alhammadi<sup>1</sup>, Weam Alhoti<sup>1</sup>, Donny Hartanto\*<sup>1,2</sup>

<sup>(1)</sup>Department of Mechanical and Nuclear Engineering, University of Sharjah, P.O. BOX 27272, Sharjah, United Arab Emirates

<sup>(2)</sup>Nuclear Energy System Simulation and Safety Research Group, Research Institute of Sciences and Engineering, University of Sharjah, P.O. BOX 27272, Sharjah, United Arab Emirates

### ARTICLE INFO

#### Article history:

Received: 14<sup>th</sup> Sept. 2021

Accepted: 16<sup>th</sup> Feb. 2022

#### Keywords:

Nuclear Thermal Rocket;

Low Enriched Uranium;

Serpent 2;

Specific Impulse;

Fuel Temperature;

Propellant Exit Temperature.

### ABSTRACT

Recent years have proven that sending humans to Mars may be challenging but not impossible. Earlier tests have proven that nuclear rockets can be more efficient than chemical rockets. In a chemical rocket, the propellant requirements are enormous, which means higher launching costs. This, in turn, will result in a longer trip time. Meanwhile, nuclear rockets have at least twice the propellant efficiency of chemical propulsion systems, allowing a reduction in propellant requirement and launching costs, decreasing the trip time by almost a half, thus, making them more desirable for beyond low earth orbital missions. In this study, a nuclear thermal rocket (NTR) was designed with U<sup>235</sup> enrichment of 19.75% to power up the rocket and produce a high specific impulse ( $I_{sp}$ ) that ranges between 850s-900s. Two different configurations were designed using Monte Carlo code Serpent 2 to test their material performance (including fuel, tie tube, and moderator) under operation. Hence, they put together an optimum configuration to withstand a harsh operating environment to achieve the mission goals. Moreover, temperature analysis was done using MATLAB to extract the power distribution from Serpent 2 to find the average value of the exit temperature for the propellant in addition to the fuel temperature and, thus, perform  $I_{sp}$  calculations. The obtained results reflected the ability of the reactor to operate at temperatures as high as 2500 K to deliver a sufficient value of  $I_{sp}$  that is equal to 864.15 s, which is a high value compared to any other convention chemical rocket.

## 1. INTRODUCTION

This study has been conducted for its promising propulsion technology, especially for beyond orbital exploration missions. The superiority of using nuclear technology lies in different areas. For starters, nuclear engines have twice the propellant efficiency of any conventional space rocket, which in return decreases the total propellant needed and launch costs [1]. In addition, nuclear engines allow to convert the excess nuclear energy to electric power during the operation, which makes these engines bimodal (propulsion and electricity generation). Nuclear thermal rockets differ from chemical rockets in terms of the heat source. Nuclear thermal rockets use a nuclear reactor to supply heat for heating the propellant to a high outlet temperature. The method is described as follows, a fluid propellant (most probably liquid hydrogen) is pumped throughout the reactor core. Inside the core, a fission reaction occurs

when the uranium atoms split away from each other. This process releases heat transferred to the propellant via convection and heats the propellant that expands, leading it to convert to a hot gas forced through the nozzle. After that, the nozzle transforms the thermal energy in the hot propellant to kinetic energy to create thrust and push the rocket into space.

The development of nuclear rockets began in the 1960s, where they were researched and developed heavily, mainly in the NERVA program by the U.S.A's. NERVA was the outcome of the Rover program that succeeded in developing the first KIWI series in 1959 thus, making it the first step in demonstrating the feasibility of developing a nuclear rocket reactor [2]. The main series of the NERVA/Rover program consisted of Kiwi-A, Kiwi-B, Phoebus-1, Phoebus-2, and Peewee [3]. Furthermore, low enriched uranium (U-235 = 19.75%) will be utilized to achieve high thrust levels, greater

power, shorter traveling time, and larger carrying payloads, eliminating any security-related issues that can arise from proliferation risks [4]. Therefore, scientists are confident that NTRs will fulfill the need for a propulsion system with a high  $I_{sp}$  and thrust. The purpose of the present investigation is to develop an NTR design that can shorten the trip duration and increase the payload compared to any chemical rocket. Furthermore, selecting the appropriate high endurance materials is also an important object that must be satisfied since all analyses will depend on the rocket's performance. On this basis, different iterations, designs, and approaches must be taken and done to accomplish an  $I_{sp}$  value higher than 850s [5].

## 2. MATERIAL SELECTION

### 2.1 Fuel

The selection of nuclear fuel for the NTR is crucial due to the extremely high operating temperatures, corrosive aqueous environment, elongated fuel cycles, irradiation effects, and high stresses due to pressurized systems. In a nuclear reactor, power is generated based on how much heat we can remove from the fuel. If all the heat is not removed, the fuel will start heating up and end up with fuel failure. Therefore, the fuel melting point must not be reached to ensure adequate rocket performance to avoid any change in the fuel geometry. As shown in Table (1), ceramic fuel options include (U,Zr)C, (U,Zr,Nb)C, (U,Zr,Ta)C, UN and UC where they have a high melting point that can reach up to 4000 K. As for the remaining fuel options, the difference between metallic fuels and metallic oxide fuels is the nature of the material. Uranium oxides are ceramic in nature, whereas uranium is metallic. This makes a significant impact on the density of the fuel and its thermal conductivity. For thermal rockets, a material with high thermal conductivity and a high melting point is most surely preferable [6].

The advantage of using ceramic fuel is its porous nature that decreases the fuel density. This point plays an important role in fuel and rocket safety. In a dense fuel, the chances of power peaking and temperatures

increasing are very high. Also, fuel atoms would be closely packed together, and the chain reaction would be fast. Therefore, using a porous fuel reduces the power produced per unit fuel volume, which means that the power peaking and the increased localized temperatures will also be reduced [7].

It is important to study the melting point temperature, thermal conductivity, and density of the selected fuel material. The fuel is chosen based on the high density of uranium to overcome the degradation of fissile material. As shown in Table (1), (U,Zr,Ta)C has the highest melting point and thermal conductivity compared to other materials, while UC has the highest density. However, ceramic fuels are preferable due to their availability and cost. Moreover, their properties match the thermal rocket properties of operating at high temperatures [4].

### 2.2 Cladding

Encapsulating the nuclear fuel rod is important to keep radioactive material isolated and avoid direct contact with the coolant. The features needed for the cladding are low absorption cross-section of the thermal neutron, high melting point, mechanical strength, the ability to handle operation with the fuel and the coolant (liquid hydrogen), and corrosion resistance.

Ceramic materials are considered as cladding for nuclear thermal rockets since they are exposed to temperatures above 1123 K [13]. Zirconium Carbide (ZrC) is the most assuring cladding material. That is due to its good chemical stability and high retention of the fission products, and a melting point of 3805 K – 3813 K [14]. Niobium Carbide (NbC) is a remarkably tough refractory ceramic material, highly corrosion-resistant, and has a high melting point of 3881 K [15]. Tungsten (W-184) can operate at a very high temperature while providing a low thermal neutron absorption cross-section. However, tungsten alone is not efficient since it is not ductile enough to coat the fuel. Thus, Rhenium (Re) is added to increase both ductility and material strength [16].

**Table (1): Thermal properties for different fuels [1, 6, 8, 9, 10, 11, 12]**

Properties	(U,Zr)C	(U,Zr,Nb)C	(U,Zr,Ta)C	UO <sub>2</sub>	UN	UC	UH <sub>3</sub>
Density (g/cm <sup>3</sup> )	16.2	12.92	12 - 13	10.97	11.3	13.63	10.95
Melting Point (K)	3813	3873	4258	2865	3110	2803	2080
Thermal Conductivity (W/m K)	10-30	20-100	20-100	1.60 -6.27	20.6	16.7 -20.9	18

### 2.3 Tie Tube

Tie tubes are used to house the moderator and they function by extracting any additional thermal energy from the reactor core. In addition, they must be made from strong structural material having a low neutron absorption cross-section. Inconel-781 is a high-strength nickel superalloy, and it was used in NERVA type reactor, and is composed mainly of nickel, chromium, and iron. Inconel-781 can operate at high temperatures that reach 1617 K [17]. TZM is an acronym for titanium, zirconium, and molybdenum. It has a higher tensile strength than pure, unalloyed molybdenum. In addition, it maintains its high strength even at higher temperatures and has a melting point of 2896 K [18]. Molybdenum alone has a high absorption cross-section which is undesirable. Thus, to reduce it, it is subjected to molybdenum (Mo-92) enrichment. Zirconium alloy has a low absorption cross-section of thermal neutrons, high hardness, ductility, and corrosion resistance. Zircaloy-4 was developed from Zircaloy-2, but it holds no nickel and has a higher, more closely controlled iron content, with the primary aim of reducing the capability to absorb hydrogen. It is similar to pure zirconium in the mechanical properties but has stronger and better corrosion resistance, and its melting point is around 2123 K [19]. Table (2) summarizes the differences between various types of tie tube materials.

### 2.4 Moderators

Since U-235 has a higher fission cross-section at thermal neutron, it has a higher probability of having a fission reaction at a lower kinetic energy (0.025 eV – 1 eV). As shown in Fig. (1, the blue line represents the fission cross-section. Moderators are used for slowing

down neutron energies from fission (1 keV – 10 MeV) to a thermal energy regime (0.025 eV – 1 eV) [7]. An efficient moderator must have a low atomic weight, which is important since it will transfer maximum energy in each collision and lead to a low number of elastic collisions to slow down the neutron. Also, a low thermal absorption cross-section is required to avoid absorbing neutrons, which leads to a decrease in the potentiality of fission. High scattering cross-section and high melting points are also important considerations [20]. To compare between the moderators, the following parameters must be defined first:

$$\text{Slowing down power} = \xi \Sigma_s \quad (1)$$

$$\text{Slowing down ratio} = \frac{\xi \Sigma_s}{\Sigma_a} \quad (2)$$

$$\Sigma_s = N \sigma_s \quad (3)$$

$$\Sigma_a = N \sigma_a \quad (4)$$

$$\xi = 1 + \frac{\left(\frac{1-A}{1+A}\right)^2}{1 - \left(\frac{1-A}{1+A}\right)^2} \ln \left( \left(\frac{1-A}{1+A}\right)^2 \right) \quad (5)$$

where  $\Sigma_s$  and  $\Sigma_a$  are the macroscopic scattering and absorption cross-section, respectively.  $\sigma_s$  and  $\sigma_a$  are microscopic scattering and absorption cross-section, respectively.  $N$  is the atom density, and  $\xi$  is the slowing down decrement, which depends solely on the atomic mass  $A$  where it can help find the number of collisions needed to slow down the neutron. From Eq. (5), it can be deduced that the atom density should not be small, so it has a large moderating effect. Based on that, gases will be neglected as a moderator. In nuclear thermal rockets, it is proposed to utilize graphite, beryllium, and metal hydride. Solid moderators are preferable for their higher density compared to the other kinds of moderators.

**Table (2): Tie tube material comparison [4]**

Properties	Inconel-781	TZM	Zircaloy 4
Density (g/cm <sup>3</sup> )	8.2	10.16	6.56
Yield Strength (Mpa)	~1200	~630	241
Melting Point (K)	~1617	2896	2123
	Ni = 4.43		
Average Cross-Section (barn)	Fe = 2.81 Cr = 3.1	Mo = 2.65	Zr = 0.111

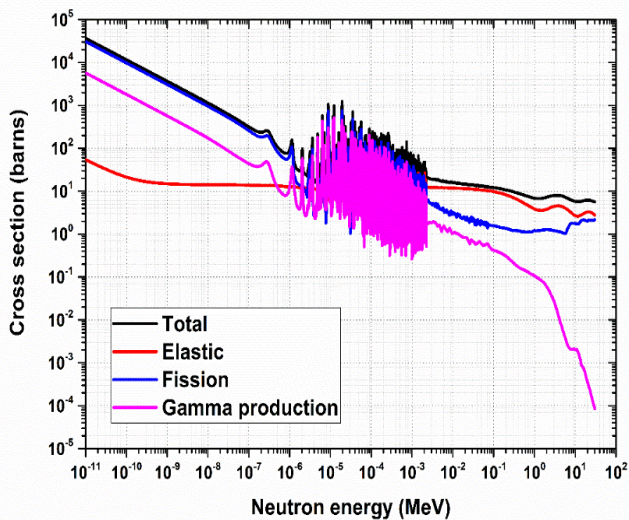


Fig. (1): U-235 cross-section [21].

Graphite has good thermal, mechanical, and heat-conducting properties, which is important for neutrons in terms of moderation and costs. It is also stable throughout a large temperature range that can reach up to 3473 K. Graphite does not melt, however, it changes from solid to vapor state directly at around 3923 K [7]. The primary drawbacks are the opportunity of oxidation in the presence of air, displacement in the crystal dimension under the effect of radiation from the reactor and being prone to non-negligible hydrogen corrosion[4].

Beryllium has less atomic weight than graphite and a high melting point of 1560 K [1], making it a good choice. However, it also has disadvantages such as high toxicity, expensive costs, and reasonably large grain size, making the metal brittle, causing surface damage [7]. In addition, beryllium exposure to fast neutrons results in

the production of helium through  $(n, \alpha)$  reactions and tritium through  $(n, 2n)$  reactions, and due to the growth of helium bubbles, it will produce high swelling, which will cause cracking [22].

Metal hydrides have been identified as an efficient, low-risk selection for high-density hydrogen storage since the late 1970s [23]. Metal hydrides are expressly suitable for thermal reactor systems where the core weight and volume are small. The most used metal hydrides that have been implied in nuclear systems applications are ( ${}^7\text{LiH}$ ,  $\text{ZrH}_x$ ,  $\text{YH}_x$ ).  ${}^7\text{LiH}$  has a low melting point (about 962 K) and low thermal conductivity, requiring a complex and efficient cooling method. In addition,  ${}^7\text{LiH}$  has a low density, and it is required to be 100% enriched of  ${}^7\text{Li}$  because a small amount of  ${}^6\text{Li}$  will cause a large reactivity penalty [24]. Moving on to  $\text{ZrH}_x$  (where  $x$  represents hydrogen to zirconium ratio), it depends on their crystallography and hydrogen composition. It has a higher operating temperature than water, low absorption cross-section, and general availability. The characteristics of  $\text{ZrH}_{1.8}$  include the following: it contains the maximum hydrogen content making it the best mechanically performing out of the other hydride options. Additionally, the structure has high strength, contributing more to the toughness [4]. Moreover, it is entirely stable under neutron irradiation but decomposes at about 1073 K, so the fuel design must be kept somewhat cool during reactor operation [7]. Lastly,  $\text{YH}_x$  is being developed under various US Department of Energy (DOE) programs to work as a moderator for micro reactors and small modular reactors. It has the advantage of thermal superiority, making it stable at high temperatures (above 1143 K), and it holds a high hydrogen content [23]. Table (3) summarizes each type of moderators and their properties.

Table (3): Candidate materials for moderators [24]

Properties	Graphite	Beryllium	${}^7\text{LiH}$	$\text{ZrH}_{1.8}$	$\text{YH}_2$
Density ( $\text{g/cm}^3$ )	2.2	1.85	0.82	5.47	4.24
Melting Point (K)	3923	1560	962	1073	-
Tensile Strength (MPa)	650	395	27.6	800	-
Thermal Conductivity ( $\text{W/m K}$ )	70	201	7.5	17	-
Slowing Down Power (1/cm)	0.06	0.16	2.97	2.90	1.2
Moderating Ratio	220.4	137.9	127.1	109.9	-

## 2.5 Control System

A reflector must be added to limit any leaking neutrons from the core, improve the neutron economy, and guarantee a smaller, more compact reactor size. The neutron reflection capabilities of both beryllium (Be) and beryllium oxide (BeO) have made them desirable candidates as reflectors in space reactors applications. The characteristics of having low densities, the lightest known structural material, a high melting point of 1553 K, and high neutron scattering cross-section and moderation serve as benefits of using these materials. To add up, both Be and BeO have a high thermal conductivity, which makes them outstanding candidates compared to other reflector options (like light water, heavy water, and graphite). However, beryllium is known for its low ductility even if irradiation is not presented, whereas BeO is considered to be relatively resistant to radiation [22].

The reflector part that surrounds the core contains the control drums. These drums play a vital role in controlling the criticality throughout the reactor core. The number of control drums varies mostly from 6 to 19, and they are distributed uniformly around the core. The design of the drums can be described as follows, one part of the drum (around 120 degrees) is coated with a material that absorbs neutrons, the standard thickness of the absorber falls between 0.5 to 1 cm. As for the remaining part (240 degrees), the drum is plated with neutron reflecting material (most probably beryllium).

To control the reactivity and thus the criticality, the neutron leakage fraction is controlled by adjusting the rotation of the control drums. For instance, to increase the reactivity, the drum is rotated so that the reflective side of each one is facing the core, which decreases the number of neutrons escaping the core [25]. The ability to control the reactivity and criticality of the reactor allows us to control the power, especially in certain cases such as reactor startup, power increase, or shut down. Fig. (2) illustrates a control system consisting of 12 control drums where the absorbing region is presented.

The reflector side of the drum primarily utilizes the same material as the reflector region that it falls in. However, on the absorber side, a combination of boron carbide (B<sub>4</sub>C) absorbers is the most presented option. Boron carbide is mainly known for its shielding properties, especially its ultra-high hardness and a melting point of 2445 K [26]. However, using B<sub>4</sub>C has its downside since the helium gas produced from the reaction can cause cracking and swelling. As for the thickness of the reflector, it is important to achieve a value that implicates an adequate operation without impacting  $k_{eff}$ .

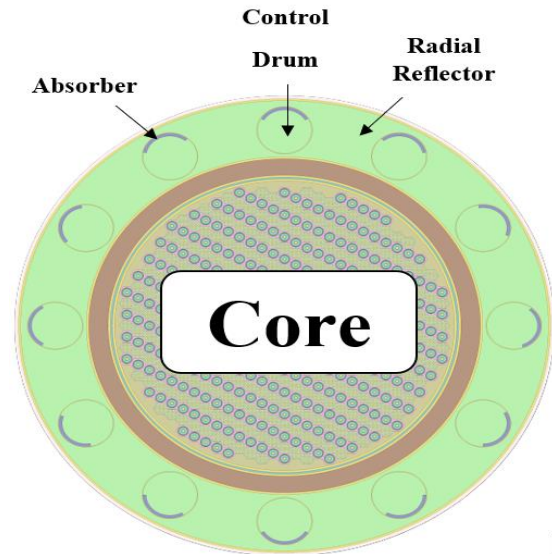


Fig. (2): Radial view of a core surrounded by a reflector that contains 12 control drums

## 3. RESULTS AND DISCUSSION

### 3.1 Reactor Core Modeling Result

Two configurations were created to compare between them by testing their performance to select the optimum configuration. Configuration 1 consisted of entire rows of fuel elements followed by entire rows of tie tubes. In contrast, configuration 2 has one fuel element followed by two tie tubes to form a complete row. The total number of fuel elements and tie tubes in configuration 1 is 280 and 287, respectively. However, in configuration 2, the total number of tie tubes is 342, and the fuel elements are 174. Also, the moderator to fuel ratio was calculated for both configurations and found to be 39.86% for configuration 1 and 19.93% for configuration 2. This ratio shows that configuration 1 has a higher moderation than configuration 2.

Fig. (3) shows the difference between both configurations.

After creating the lattice, axial layers were added to the core. The layers contained Zircaloy - 4, ZrC, and BeO. Then, the core was layered radially with 304 stainless steel, Be, and Al. Followed by that, the thickness of the reflector that housed 12 control drums with an absorber thickness of 0.5 cm was set to 9.732 cm.

Fig. (4) displays the radial and axial views in configuration 1. In addition, radial and axial dimensions are shown in Table (4). Using this configuration, the core can achieve a lifetime of about 90 days.

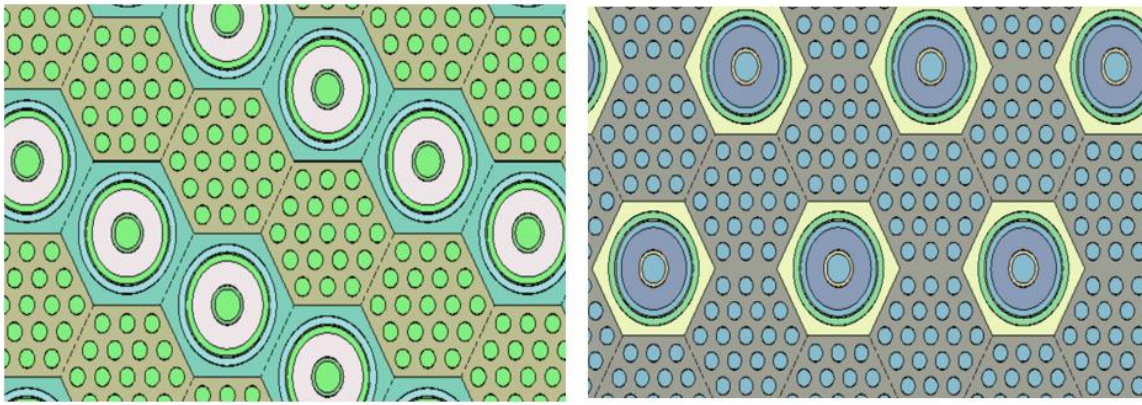


Fig. (3): Difference between configuration 1 (left) and configuration 2 (right)

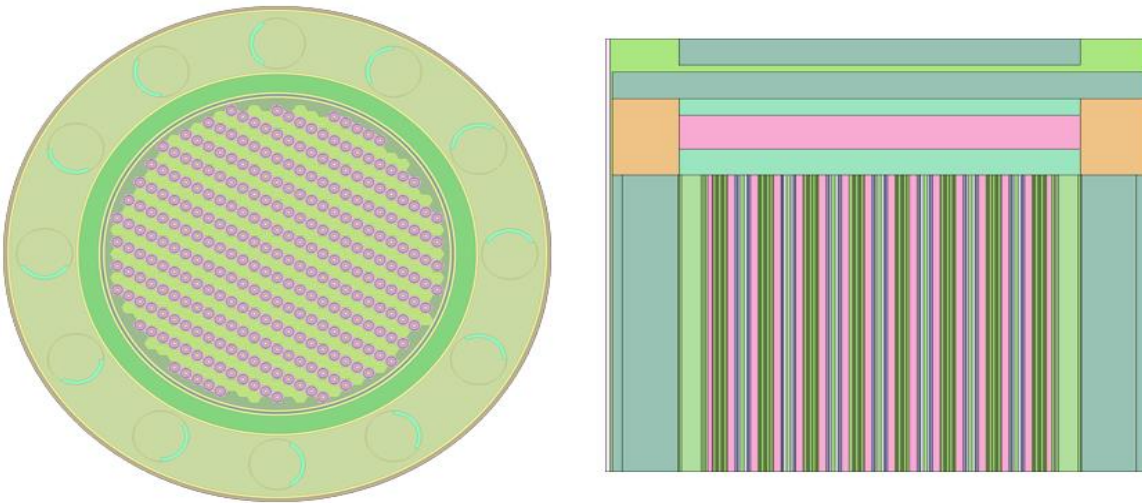


Fig. (4): Radial (left) and axial (right) view in configuration 1

Table (4): Dimensions of the nuclear thermal rocket

Region	Radius (cm)	Length (cm)
Axial region		
Core	25	-
Gap (H <sub>2</sub> )	25.3175	-
Stainless Steel 304	25.6350	-
Gap (H <sub>2</sub> )	25.9525	-
Beryllium barrel	28.8100	-
Gap (H <sub>2</sub> )	29.1275	-
Radial reflector (BeO)	38.8595	-
Gap (H <sub>2</sub> )	39.1770	-
Pressure vessel (Al)	39.7358	-
Radial region		
Core		89
Lower tie tube (Zr-4)		96.62
Core support plate (ZrC)		106.78
Upper tie tube (Zr-4)	29.1275	111.860
Lower internal shield (BeO)		119.734
Hydrogen plenum		121.766
Upper internal shield (BeO)		129.640

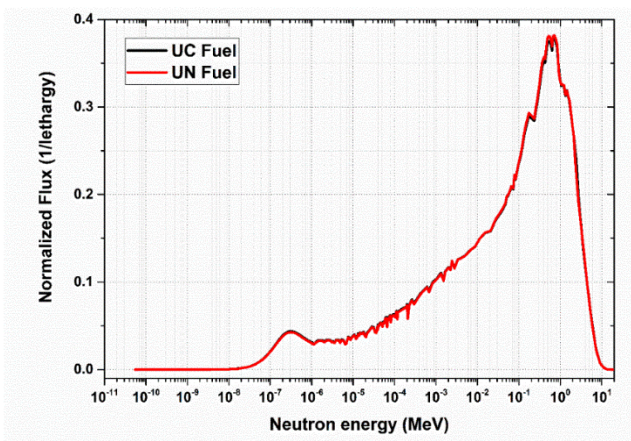
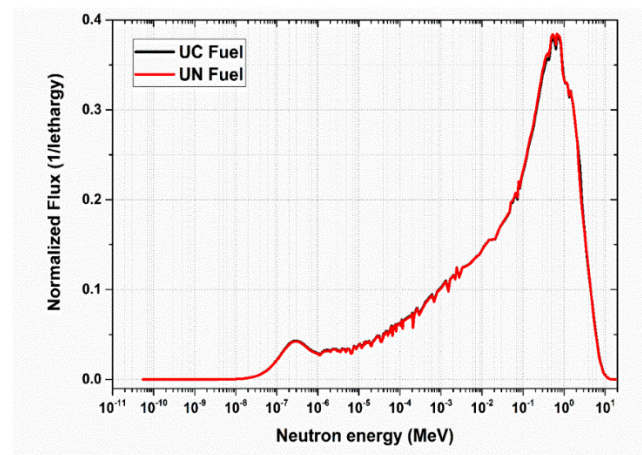
### 3.2 Material Selection Result

Starting with the fuel, four types were selected to be tested in configurations 1 and 2. The tests were conducted for UO<sub>2</sub>, UN, UC, and UH<sub>3</sub>. The results of UO<sub>2</sub> and UH<sub>3</sub> fuel proved to be unsatisfactory for the operation. First, UO<sub>2</sub> gave a value of  $k_{eff}$  less than 1, which is not enough to sustain a fission reaction. As for the UH<sub>3</sub>,  $k_{eff}$  was unacceptably high. However, UH<sub>3</sub> needs an additional component for the reactor to maintain the hydrogen pressure since it has low decomposition at a high temperature. The remaining options (UC and UN) performed well in endurance to high temperatures and criticality. Several moderator options were included, such as ZrH<sub>1.8</sub>, LiH, and YH<sub>2</sub>. YH<sub>2</sub> was the first option to be eliminated for bringing the system to subcriticality to use UC as fuel. As for ZrH<sub>1.8</sub> and LiH, their results showed that both follow the same behavior.

**Table (5): Criticality results for configurations one and two**

Fuel	Moderator	Tie Tube	$k_{\text{eff}}$ Configuration 1	$k_{\text{eff}}$ Configuration 2
UC	ZrH <sub>1.8</sub>	Inconel-781	1.01362 ± 0.00025	1.00307 ± 0.00024
		Zircaloy 4	1.02111 ± 0.00024	1.00584 ± 0.00021
	LiH	Inconel-781	1.01388 ± 0.00024	1.00456 ± 0.00021
		Zircaloy 4	1.02040 ± 0.00026	1.00722 ± 0.00024
UH <sub>3</sub>	ZrH <sub>1.8</sub>	Inconel-781	0.99385 ± 0.00025	0.99276 ± 0.00023
		Zircaloy 4	1.20825 ± 0.00021	1.19109 ± 0.00024
	LiH	Inconel-781	1.22101 ± 0.00023	1.19723 ± 0.00021
		Zircaloy 4	1.22140 ± 0.00022	1.19810 ± 0.00021
UN	ZrH <sub>1.8</sub>	Inconel-781	1.19662 ± 0.00022	1.19142 ± 0.00023
		Zircaloy 4	1.02083 ± 0.00026	1.01264 ± 0.00024
	LiH	Inconel-781	1.02759 ± 0.00022	1.01476 ± 0.00023
		Zircaloy 4	1.02173 ± 0.00024	1.01417 ± 0.00023
UO <sub>2</sub>	YH <sub>2</sub>	Inconel-781	1.02765 ± 0.00023	1.01641 ± 0.00022
		Zircaloy 4	1.00174 ± 0.00025	1.00257 ± 0.00024
	ZrH <sub>1.8</sub>	Inconel-781	0.94716 ± 0.00027	0.91010 ± 0.00024
		LiH	Inconel-781	0.92296 ± 0.00028
	YH <sub>2</sub>	Inconel-781	0.94765 ± 0.00028	0.89673 ± 0.00025

The moderator is housed between the inner tie tube and the outer tie tube. The results for using Zircaloy - 4 as the material for the tie tube showed a slightly higher criticality than using Inconel-781. Table (5) displays the results in both configurations 1 and 2 after testing different materials for the fuel, moderator, and tie tube. Generally, configuration 1 gave higher values of  $k_{\text{eff}}$  compared to configuration 2. Therefore, configuration 1 was selected with pursuing UN and UC fuels.

**Fig. (5): Flux distribution for LiH moderator with UC and UN fuel****Fig. (6): Flux distribution for ZrH<sub>1.8</sub> moderator with UC and UN fuel**

As for the moderator, Fig. (5) and Fig. (6) show the flux distribution of LiH and ZrH<sub>1.8</sub> with UN and UC fuels. Both moderators have no difference in their thermalization characteristics. Hence, LiH was selected due to its lower density ( $\rho = 0.82 \text{ g/cm}^3$ ) which will result in a lighter more compact reactor. And finally, Zircaloy 4 was selected for the tie tube for its effect of slightly increasing the value of  $k_{\text{eff}}$ .

The thermal peak could be enhanced by improving the moderation characteristics. For this case, the moderator radius was expanded slightly step by step. Table (6) shows how the criticality increases with increasing moderation. This can also be illustrated in Fig. (7), where the thermal peak deliberately enhances as well. Comparing the results, the moderator radius of 0.62500 cm was determined to be the optimum one.

**Table (6): Criticality changes with moderator radius**

Test	Moderator Radius (cm)	K-eff
0	0.58420	1.02765 ± 0.00023
1	0.62500	1.03529 ± 0.00025
2	0.74612	1.11828 ± 0.00023
3	0.83375	1.17447 ± 0.00021

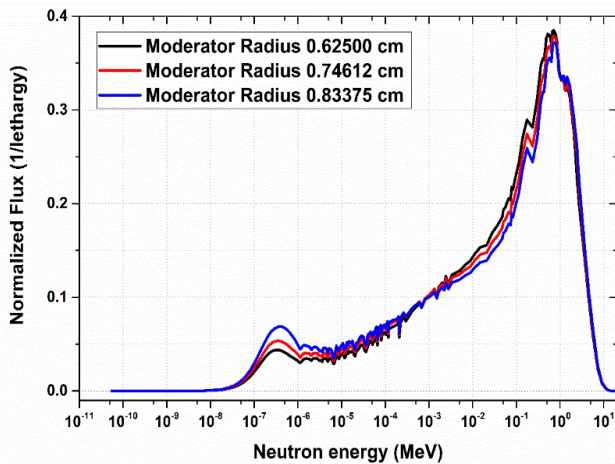


**Fig. (7): Flux distribution for various moderator radius**

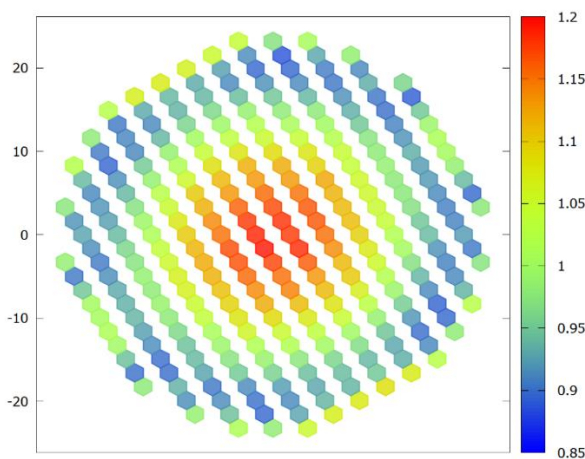


**Fig. (8): Radial power distribution**

After selecting the final configuration with the appropriate materials, the axial and radial power distribution were estimated to display how the power is

distributed along the coordinates. The axial power distribution has a power peaking factor of 1.38, whereas, in the radial, the power peaking factor is 1.24. Fig. (8) and Fig. (9) show how in both distributions, the power is concentrated at the center of the reactor core and decreases as we move outwards. However, it was noticed that the upper part of the axial power distribution is cropped due to the introduced layers limiting neutron losses.

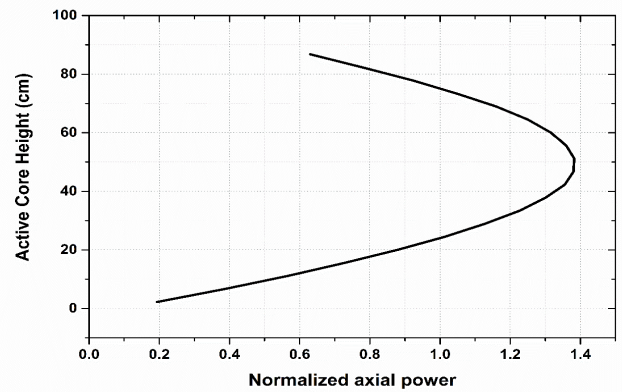


**Fig. (9): Axial power distribution**

### 3.3 Fuel and Moderator Temperature Coefficient

One of the important reactivity-related safety features that maintain a stable reactor is the temperature coefficient of the fuel and moderator. It is defined as the change of reactivity with changing the temperature of either the fuel or the moderator. The fuel temperature coefficient (FTC) depends on the enrichment and the fuel burn-up and is given by Eq. (6) [20]. FTC was found to be -1.48451 pcm/K, which means that any temperature change in the fuel will cause a reactivity decrease.

$$\alpha_T = \frac{d\rho}{dT_F} \tag{6}$$

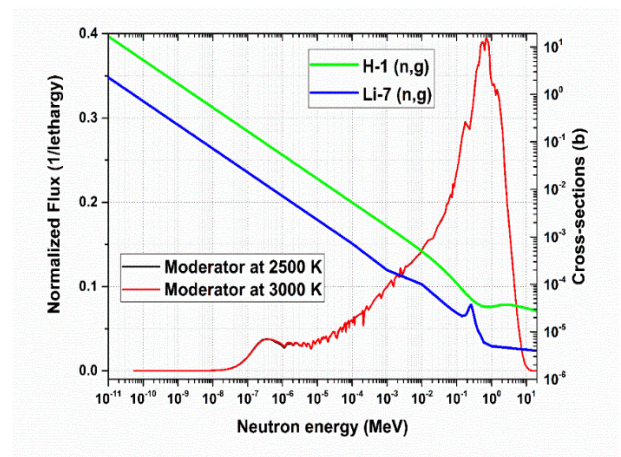


**Fig. (10) Flux behavior with moderator cross-section**

The moderator temperature coefficient (MTC) is given by Eq. (7) [20] and is primarily a function of the moderator-to-fuel ratio. The resulted value was 0.23207 pcm/K. Getting a positive number results in an unstable system that affects the safety of the reactor. This issue can be mitigated with a significant negative FTC value. According to Fig. (10, increasing the temperature makes the spectra slightly hardening, and the capture cross-section for the moderator is reduced. This justifies the positive value of MTC.

$$\alpha_M = \frac{d\rho}{dT_M} \quad (7)$$

### 3.4 Temperature analysis

To get the temperature at each coordinate, all constants were provided in Table (7, where  $R_i$  is channel inner radius,  $R_o$  is fuel element radius [27],  $T_{in}$  is inlet temperature,  $\dot{m}$  is coolant mass flow rate, and  $C_p$  represents hydrogen specific heat which is a function of temperature [28]. The mass flow rate was initially 3.76 kg/s according to the NERVA design [29]. Then iterations for  $\dot{m}$  were conducted to find a suitable outlet temperature for the propellant, and it was found to be  $\dot{m} = 5.54$  kg/s that resulted in  $T_p = 2473.5$  K using equation (8) [7]. Fig. (11 illustrates the outlet temperature for the propellant for each fuel element.

$$T_p(z) = T_{in} + \left( \frac{p(z)}{\dot{m}C_p} \right) \quad (8)$$

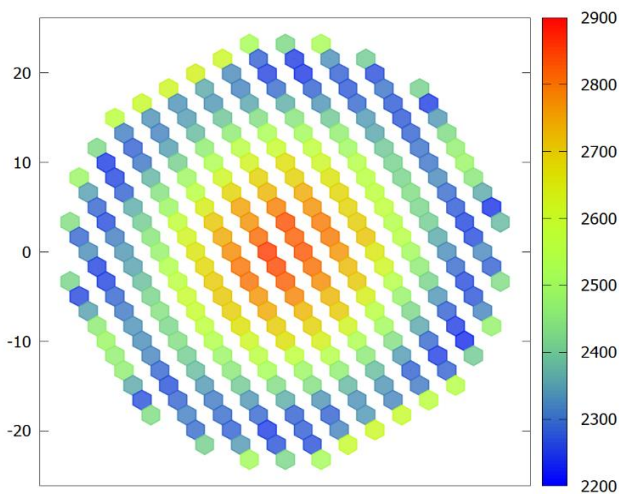


Fig. (11): Outlet temperature distribution for the propellant at each fuel element

Moreover, the fuel temperature was calculated using equation (9) [7], where  $D_h$  is the hydraulic diameter of the flow channel,  $h_c$  is heat transfer coefficient,  $k$  is thermal conductivity,  $m_u$  is fluid viscosity,  $N_u$  is Nusselt Number,  $P_r$  is Prandtl number, and  $Re$  is Reynold

number. Finally,  $N_u$  and  $h_c$  were calculated using equations (10) and (11), respectively [7].

$$T_f(z) = T_p(z) + P(z) \left\{ \frac{r_o^2 - r_i^2}{2h_c r_i} - \frac{1}{2K} \left[ \frac{r_o^2 - r_i^2}{2} + r_o^2 \ln \left( \frac{r_i}{r} \right) \right] \right\} \quad (9)$$

$$N_u = 0.023 Re^{0.8} Pr^{0.4} \quad (10)$$

$$h_c = \frac{N_u K}{D} \quad (11)$$

As for  $m_u$  and  $k$ , both are temperature- dependent [28]. The results achieved was  $T_f = 2161.3$  K, which is in the hottest region of the core. Based on the fuel's outlet temperature, it is guaranteed that the reactor operates at a temperature lower than its melting temperature. Fig. (12) shows how the fuel temperature is distributed along the z-axis.

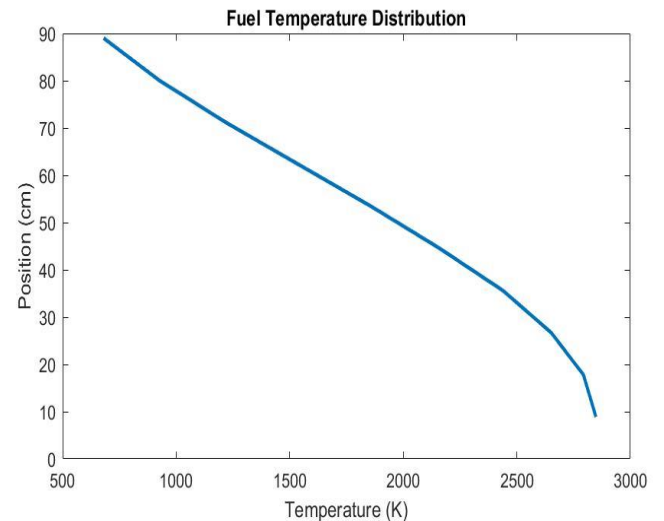


Fig. (12): Fuel temperature along the z-axis

### 3.5 $I_{sp}$ Calculation

All analyses performed to get the exit temperature of the propellant were for the sole purpose of calculating the  $I_{sp}$ , which will give an insight into the rocket's performance and efficiency.  $I_{sp}$  was calculated using equation (12) where  $R_u$  is the universal gas constant,  $g$  is gravitational acceleration,  $A$  is propellant molecular weight [7], and  $T_p = 2473.5$  K. In addition,  $\gamma$  is specific heat ratio for hydrogen was calculated using equation (13) [7].

$$I_{sp} = \frac{1}{g} \sqrt{\frac{2\gamma}{\gamma-1} \frac{R_u}{A} T_p \left( 1 - \left( \frac{P_e}{P_c} \right)^{\frac{\gamma-1}{\gamma}} \right)} \quad (12)$$

$$\gamma = \frac{c_p}{c_p - (R_u/c_p)} \quad (13)$$

Since  $P_e/P_c$  is required to obtain the  $I_{sp}$ , it was calculated and found to be equal to  $5.3230 \times 10^{-5}$ . This term was found from the Mach number, which is dependent on the nozzle area ratio. From the small NERVA, this ratio is given to be 300 [29]. With all the required constants and data,  $I_{sp}$  was calculated and found to be 864.15 sec. Another approach for calculating the  $I_{sp}$  was implemented. In this case, since the rocket will be operating in the vacuumed environment, an assumption to make the exit pressure zero was made. Therefore, the term  $P_e/P_c$  was neglected, and calculations were carried finding that  $I_{sp}$  is 864.16 sec for this case. All data are summarized and displayed in Table (7).

**Table (7): Parameters used in temperature and  $I_{sp}$  analyses**

Parameter	Value
$R_i$ (cm)	0.1285
$R_o$ (cm)	0.20545
$T_{in}$ (K)	453
$\dot{m}$ (kg/s)	5.54
$C_p$ (J/kg-K)	14517.53
Reactor Thermal Power (MW)	161.6
$T_p$ (K)	2473.5
$D_h$ (cm)	0.1539
$k$ (W/cm.K)	0.1980
$m_u$ (Pa.s)	$9.999 \times 10^{-6}$
$P_r$ number	0.7331
$R_e$ number	$4.5838 \times 10^6$
$N_u$ number	$4.3328 \times 10^3$
$h_c$ (W/cm <sup>2</sup> -K)	$5.5749 \times 10^3$
$T_f$ (K)	2161.3
$R_u$ (J/kg-K)	8314
$g$ (m/s <sup>2</sup> )	9.8067
$A$ (g/mole)	2
$\gamma$	1.4
$I_{sp}$ (sec)	864.16

#### 4. CONCLUSIONS

To sum up, many steps were taken to reach a suitable value of  $I_{sp}$  that defines the performance of the reactor on a smaller scale and the rocket in a bigger one. In this study, the small NERVA design was approached as the reference prototype. Furthermore, extensive studies were performed to see which materials can withstand such a harsh operating environment, only to select the best ones

that can be used in the optimum configuration (configurations 1). The final selected materials consisted of UN fuel with enrichment of 19.75% for its higher criticality, and a LiH moderator housed in the Zircaloy-4 tie tube. Through this process, not only different materials were tested, but also the size of certain reactor parts (moderator, reflector, tie tube, and control drums) was adjusted several times to achieve an adequate rocket performance. Both the axial and radial power distribution were illustrated to observe their behavior throughout the reactor core, in addition to the flux distribution where we can observe the change in the thermal peak with varying moderator sizes. Then, by completing the reactor design, an appropriate fuel temperature was achieved by performing different iterations for the mass flow rate to ensure that the operating temperature will not exceed the fuel's melting point temperature. By guaranteeing a safe operation, the  $I_{sp}$  was then calculated using the propellant outlet temperature and was found to be 864.15, which reflects how efficient is the achieved configuration. Moreover, the reactor geometry and the material testing were done using Serpent 2, which helped discover areas such as the flux and power distribution throughout the reactor core in addition to the criticality achieved.

#### ACKNOWLEDGMENT

This research was supported by Undergraduate Student Project Funding, the Office of Vice Chancellor for Research & Graduate Studies, University of Sharjah.

#### REFERENCES

- [1] Nam, S., Venneri, P., Kim, Y., Lee, J., Chang, S., & Jeong, Y. (2015). Innovative concept for an ultra-small nuclear thermal rocket utilizing a new moderated reactor. *Nuclear Engineering and Technology* 47, 678-699
- [2] Esselman, W. (1965) The NERVA nuclear rocket program. *Westinghouse Engineer* 25 (3), 66-75
- [3] Benensky, K. (2013). *Summary of Historical Solid Core Nuclear Thermal Propulsion Fuels*. Pennsylvania: Penn State Nuclear Engineering Society.
- [4] Venneri, P. F. and Kim, Y. (2015) A feasibility study on low-enriched uranium fuel for nuclear thermal rockets - I: Reactivity Potential, *Progress in Nuclear Energy* 83, 406-418.
- [5] Palomares, K., Howard, R., & Steiner, T. (2020). Assessment of near-term fuel screening and qualification needs for nuclear thermal propulsion systems. *Nuclear Engineering and Design* 367, 110765.

- [6] Neupane, G. (2019) Low Enriched Uranium based Nuclear Rocket Propulsion Technology: Mars Exploration Mission, *International Journal of Research and Engineering* 6 (1), 569-574.
- [7] Emrich, J. W. (2016). *Principles of Nuclear Rocket Propulsion*. Butterworth-Heinemann.
- [8] Sterbentz, J. W., Werner, J. E., Hummel, A. J., Kennedy, J. C., O'Brien, R. C., Dion, A. M., . . . Ananth, K. P. (2018). *Preliminary Assessment of Two Alternative Core Design Concepts for the Special Purpose Reactor*. United Kingdom: Idaho National Lab - USDOE Office of Nuclear Energy.
- [9] Lee, H., Lim, H., Han, T., & Čerba, Š. (2015). A neutronic feasibility study on a small LEU fueled reactor for space applications. *Annals of Nuclear Energy* 77 , 35-46.
- [10] Masrukan, Yanlinastuti, Alhasa, M. H., & Sasongko, A. (2019). Analysis of Composition, Density, and Thermal Properties of U-Zr-Nb Alloy Powder for Nuclear Fuel. *Journal of Physics Conference Series* 1198.
- [11] Knight, T., & Anghaie, S. (1999). Ternary Carbide Uranium Fuels For Advanced Reactor Design Applications. *Innovative Nuclear Space Power and Propulsion Institute*.
- [12] Khandaq, M. F., Harto, A. W., & Agung, A. (2020). Conceptual core design study for Indonesian Space Reactor (ISR). *Progress in Nuclear Energy* 118, 103109.
- [13] Azevedo, C.R.F. (2011). Selection of fuel cladding material for nuclear fission reactors, *Engineering Failure Analysis* 18 (8), 194301962.
- [14] *Zirconium carbide*. (2021, February 4). Retrieved from Wikipedia, the free encyclopedia: [https://en.wikipedia.org/wiki/Zirconium\\_carbide#:~:text=Due%20to%20the%20presence%20of%20metallic%20bonding%2C%20ZrC,high%20modulus%20%28~440%20GPa%29%20and%20hardness%20%2825%20GPa%29](https://en.wikipedia.org/wiki/Zirconium_carbide#:~:text=Due%20to%20the%20presence%20of%20metallic%20bonding%2C%20ZrC,high%20modulus%20%28~440%20GPa%29%20and%20hardness%20%2825%20GPa%29)
- [15] *Niobium carbide*. (2021, August 22). Retrieved from Wikipedia, the free encyclopedia: [https://en.wikipedia.org/wiki/Niobium\\_carbide](https://en.wikipedia.org/wiki/Niobium_carbide)
- [16] El-Genk, M. S. and Tournier, J. M. (2005). A review of refractory metal alloys and mechanically alloyed-oxide dispersion strengthened steels for space nuclear power systems, *Journal of Nuclear Materials* 340 (1), 93-112.
- [17] *Inconel 781 technical data*. (2015). Retrieved from: <https://www.hightempmetals.com/techdata/hitemplinconel718data.php>
- [18] *TZM molybdenum*. (2020). Retrieved from: <https://www.molybdenum.com/materials/tzm-molybdenum/>
- [19] *Zirconium alloy - zircaloy-4*. (2020). Retrieved from: <https://www.nuclear-power.net/nuclear-engineering/metals-what-are-metals/alloys-composition-properties-of-metal-alloys/zirconium-alloys/zirconium-alloy-zircaloy-4/>
- [20] Lewis, E. (2008). *Fundamentals of Nuclear Reactor Physics*. Academic Press.
- [21] ENDF/B-VII.1 Incident-Neutron Data. (2011). Retrieved from: <https://t2.lanl.gov/nis/data/endl/endlvii.1-n.html>
- [22] Snead, L. and Zinkle, S. (2005). Use of Beryllium and Beryllium Oxide in Space Reactors, *AIP Conference Proceedings* 746 (1), 768.
- [23] Hu, X., Schappel, D., Silva, C., and Terrani, K. (2020) Fabrication of yttrium hydride for high-temperature moderator application, *Journal of Nuclear Materials* 539, 152335.
- [24] Nam, S., Venneri, P., Kim, Y., Chang, S., and Jeong, Y. (2016) Preliminary conceptual design of a new moderated reactor utilizing an LEU fuel for space nuclear thermal propulsion, *Progress in Nuclear Energy* 91, 183-207.
- [25] Hasse, A., Smith, M., Pershke, B., Adams, A. and Gilliam, S. (2016) Control System Requirements for a Nuclear Thermal Propulsion System, Chancellor's Honors Program Projects, University of Tennessee, Knoxville.
- [26] Wu, Y., Cao, Y., Wu, Y. and Li, D. (2020). Neutron Shielding Performance of 3D-Printed Boron Carbide PEEK Composites, *Materials (Basel)* 13(10), 2314.
- [27] Akyuzlu, K. M. (2015). Numerical study of high temperature and high velocity gaseous hydrogen flow in a cooling channel of a nuclear thermal rocket core. *Journal of Nuclear Engineering and Radiation Science* 1, 2332-8983.
- [28] Appel, B. (2012). *Multiphysics Design and Simulation of a Tungsten-Cermet Nuclear Thermal Rocket*. Master's Thesis, Texas A&M University.
- [29] Belair, M. L., Sarmiento, C. J., and Lavelle, T. M. (2013). *Nuclear thermal rocket simulation in NPSS*. Proceedings of 49<sup>th</sup> AIAA/ASME/SAE/ASEE Joint Propulsion Conference, San Jose, CA, July 14 – 17